DJ-1 regulates the integrity and function of ER-mitochondria association through interaction with IP3R3-Grp75-VDAC1

Yi Liu[a,b], Xiaopin Ma[b], Hisashi Fujioka[c], Jun Liu[a,1], Shengdi Chen[a,1], and Xiongwei Zhu[b,1]

[a]Department of Neurology and Collaborative Innovation Center for Brain Science, Ruijin Hospital, Shanghai Jiao Tong University School of Medicine, 200020 Shanghai, People's Republic of China; [b]Department of Pathology, Case Western Reserve University, Cleveland, OH 44106; and [c]Electron Microscopy Core Facility, Case Western Reserve University, Cleveland, OH 44106

Edited by Solomon H. Snyder, Johns Hopkins University School of Medicine, Baltimore, MD, and approved October 31, 2019 (received for review April 16, 2019)

Loss-of-function mutations in DJ-1 are associated with autosomal recessive early onset Parkinson's disease (PD), yet the underlying pathogenic mechanism remains elusive. Here we demonstrate that DJ-1 localized to the mitochondria-associated membrane (MAM) both in vitro and in vivo. In fact, DJ-1 physically interacts with and is an essential component of the IP3R3-Grp75-VDAC1 complexes at MAM. Loss of DJ-1 disrupted the IP3R3-Grp75-VDAC1 complex and led to reduced endoplasmic reticulum (ER)-mitochondria association and disturbed function of MAM and mitochondria in vitro. These deficits could be rescued by wild-type DJ-1 but not by the familial PD-associated L166P mutant which had demonstrated reduced interaction with IP3R3-Grp75. Furthermore, DJ-1 ablation disturbed calcium efflux-induced IP3R3 degradation after carbachol treatment and caused IP3R3 accumulation at the MAM in vitro. Importantly, similar deficits in IP3R3-Grp75-VDAC1 complexes and MAM were found in the brain of DJ-1 knockout mice in vivo. The DJ-1 level was reduced in the substantia nigra of sporadic PD patients, which was associated with reduced IP3R3-DJ-1 interaction and ER-mitochondria association. Together, these findings offer insights into the cellular mechanism in the involvement of DJ-1 in the regulation of the integrity and calcium cross-talk between ER and mitochondria and suggests that impaired ER-mitochondria association could contribute to the pathogenesis of PD.

mitochondrial dysfunction | ER-mitochondria association | DJ-1 | Parkinson's disease | IP3R3

Parkinson's disease (PD) is the second most common neurodegenerative disease, which is characterized by selective and extensive loss of dopaminergic neurons in the substantia nigra and accumulation of intraneuronal inclusions, called Lewy bodies, consisting mainly of highly ubiquitinated α-synuclein aggregates in the surviving neurons (1–3). Despite intensive research efforts in the field, the pathogenic mechanism of this devastating disease remains elusive, which impedes the development of effective therapeutics. The majority of PD cases are sporadic, and less than 10% are familial forms caused by genetic mutations in a dozen genes including dominant mutations in *SNCA*, *LRRK2*, and *VPS35* genes encoding α-synuclein, LRRK2, and VPS35, respectively, and recessive mutations in *PINK1*, *PARK2*, and *PARK7* genes encoding PINK1, Parkin, and DJ-1, respectively (4). Studies into the functions of these familial PD (fPD)-related proteins contribute significantly to our current understanding of the disease (5, 6).

Recently, a potential role of disturbed endoplasmic reticulum (ER)-mitochondria association is increasingly implicated during neurodegeneration (7). ER-mitochondria association is a specialized tight structural association between a closely apposed ER surface and an outer mitochondria membrane that regulates a variety of essential physiological functions ranging from calcium signaling, phospholipid synthesis/exchange, mitochondrial biogenesis and dynamics, and autophagy to cell death (8). Many of these functions have been altered during neurodegeneration, and it is suggested that disturbed ER-mitochondria association may serve as a common convergent neurodegenerative mechanism (7, 9, 10). Indeed, increasing evidence has demonstrated that many of the fPD-related proteins are localized to mitochondrial-associated ER membrane (MAM) and impact ER-mitochondria association and function (11–15).

Missense, truncation, and splice site mutations in DJ-1 associated with loss of function lead to an autosomal recessive, early onset fPD (4). DJ-1 is a conserved multifunctional protein implicated in different cellular processes, but the specific role of DJ-1 in the pathogenesis of PD is still unclear. Earlier studies demonstrated mitochondrial localization of DJ-1 (16). Since then, many studies have demonstrated that DJ-1 is a crucial regulator of mitochondrial dynamics and integrity (17–19). On the other hand, a possible role of DJ-1 in ER and mitochondrial calcium homeostasis has also been described (20–22). In this regard, given the well-known function of ER-mitochondria association in the regulation of mitochondrial dynamics and the calcium signaling between the ER and mitochondria, like other PD-related factors (13, 23, 24), a potential role for DJ-1 in the regulation of ER-mitochondria contacts and function warrants detailed scrutiny. In this study, we aimed to determine whether DJ-1 deficiency can cause deficits in the integrity and function of ER-mitochondria association and explore the potential underlying mechanism.

Results

DJ-1 Ablation Disrupt ER-Mitochondria Association. fPD-associated DJ-1 mutations likely result in loss of DJ-1 function (4). Three

Significance

Endoplasmic reticulum (ER) and mitochondria form close associations that serve as a critical signaling platform. Loss-of-function mutations in DJ-1 are associated with autosomal recessive early onset Parkinson's disease (PD). We found that DJ-1 knockout caused significant impairments in the structure and function of ER-mitochondria association in neuronal cells and in vivo. Reduced DJ-1 was associated with deficits in ER-mitochondria association in the substantia nigra of sporadic PD. Our study identifies DJ-1 as a critical component of the macrocomplex containing IP3R3-Grp75-VDAC1 at mitochondria-associated membrane and as playing an important role in the regulation of the integrity and function of ER-mitochondria association. Our research offers insights into the regulation mechanism of ER-mitochondria association and the pathogenic mechanism of DJ-1 deficiency in PD.

Author contributions: Y.L., J.L., S.C., and X.Z. designed research; Y.L., X.M., and H.F. performed research; Y.L., J.L., S.C., and X.Z. analyzed data; and X.Z. wrote the paper.

The authors declare no competing interest.

This article is a PNAS Direct Submission.

[1]To whom correspondence may be addressed. Email: xiongwei.zhu@case.edu, jly0520@hotmail.com, or chensd@rjh.com.cn.

This article contains supporting information online at https://www.pnas.org/lookup/suppl/doi:10.1073/pnas.1906565116/-/DCSupplemental.

First published November 25, 2019.

independent clones of stable DJ-1 knockout M17 cell lines (DJ-1 KO cells) were established (*SI Appendix*, Fig. S1) using the CRISPR/Cas9 gene-editing method to study the pathogenic mechanism of loss of DJ-1 function in PD. There was no increase in basal cell death in KO cells compared with control cells. To explore a potential role of DJ-1 in the regulation of ER-mitochondria association, we performed a quantitative electron microscopy analysis of ER-mitochondria association by determining the number, length, thickness, and proportion of the mitochondrial surface that was closely apposed to ER with a distance less than 30 nm. Approximately 6.10 ± 0.86% of the mitochondrial surface was closely apposed to ER in control M17 cells; however, this proportion significantly decreased to around 3.58 ± 0.37% in the DJ-1 KO M17 cells (Fig. 1 *A* and *B*). The proportion of shorter ER-mitochondria association (<200 nm) was increased while the proportion of longer ones (200 to 400 nm and >400 nm) dramatically decreased (*SI Appendix*, Fig. S2*B*), which resulted in a significant reduction in the average length of ER-mitochondria association in DJ-1 KO M17 cells (136.3 ± 8.66 nm) compared with control M17 cells (187.3 ± 19.31 nm) (Fig. 1*C*). No changes in the thickness were noted (*SI Appendix*, Fig. S2*A*).

We then evaluated the functional changes in the DJ-1 KO M17 cells by determining the ER-mitochondria calcium transfer. To this end, M17 cells were infected with the mitochondria matrix-targeted Ca^{2+} fluorescent sensor CEPIA4, and mitochondrial Ca^{2+} uptake following histamine treatment was measured. Histamine treatment led to an increase in mitochondrial Ca^{2+} levels, the peak of which was significantly lower in the DJ-1 KO M17 cells (Fig. 1*D*), suggesting an impaired mitochondrial calcium uptake upon histamine treatment in the DJ-1 KO cells. ER Ca^{2+} changes generated by histamine treatment were further carried out using the ER lumen-targeted Ca^{2+} fluorescent sensor GECO protein. The release of calcium from ER stores after histamine stimulation was also significantly impaired in DJ-1 KO cells (Fig. 1*E*) since the ER calcium signal of DJ-1 KO cells dropped significantly less than that of control cells. ATP production also significantly decreased in DJ-1 KO M17 cells (Fig. 1*F*), suggesting mitochondrial dysfunction.

DJ-1 Is a MAM Protein. To explore how DJ-1 is involved in the regulation of ER-mitochondria association, we first determined whether DJ-1 is present in the MAM, a specialized subdomain

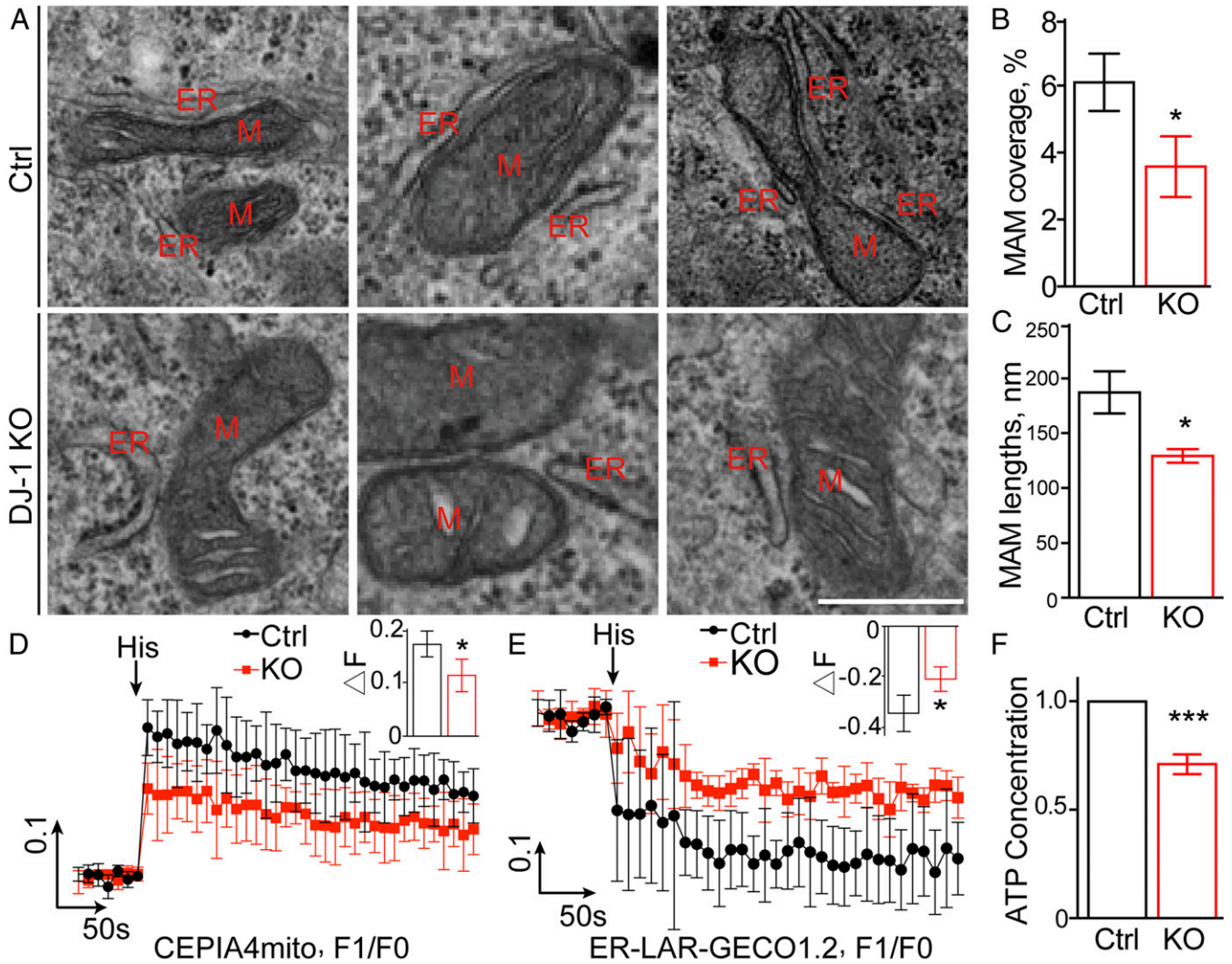

Fig. 1. DJ-1 ablation reduced ER-mitochondria association and disrupted mitochondrial calcium upload and ATP production. (*A*) Representative electron micrographs of ER-mitochondria association in control and DJ-1 KO M17 cells. M, mitochondria, ER, endoplasmic reticulum. (Scale bar, 500 nm.) (*B* and *C*) Quantitative analysis of percentage of the mitochondrial surface closely apposed to ER (*B*) and average length (*C*) of ER-mitochondria association in control ($n = 9$) and DJ-1 KO M17 cells ($n = 6$). (*D* and *E*) Representative curves of the time scan of mitochondrial Ca^{2+} (*D*) and ER Ca^{2+} (*E*) after histamine (His) treatment in control and DJ-1 KO M17 cells of 4 independent experiments. (*Inset* graph) Maximal mitochondrial (*D*) or ER (*E*) Ca^{2+} peak fluorescence. (*F*) Intracellular ATP concentration in control and DJ-1 KO cells. Data are means ± SD based on 3 independent experiments, Student *t* test; $*P < 0.05$; $***P < 0.001$.

between the ER and mitochondria that is involved in the cross-talk between the 2 organelles (Fig. 2*A*). Percoll-based subcellular fractionation of normal M17 cells was performed to collect fractions of mitochondria, ER, and MAM, and the identity and purity of each fraction were confirmed by Western blot analysis with organelle-specific markers such as Calnexin and Sigma 1 Receptor for both ER and MAM, with Grp75 and VDAC1 for both mitochondrial and MAM, with COX IV for mitochondria only. Endogenous DJ-1 is found in the crude mitochondrial preparation which contains both mitochondria and MAM. Importantly, endogenous DJ-1 is found in the MAM fractions. Pure mitochondrial fractions are effectively removed from the final MAM fractions because COX IV is not detected in the MAM factions. We found that DJ-1 is also present in the MAM in vivo in the brains of both mice and humans (Fig. 2 *B* and *C*).

To investigate whether DJ-1 is involved in the contact formation between mitochondria and ER, an in vitro ER-mitochondria contact formation assay was performed (25, 26). Pure mitochondria and microsome were independently isolated from control and DJ-1 KO cells and then incubated together for 30 min at 37 °C to allow the formation of contacts between mitochondria and ER. Mitochondria were reisolated by centrifugation, and coprecipitated microsome was determined by Western blot analysis with Calnexin. Compared to that of both mitochondria and microsome from control cells, the amount of microsome bound to mitochondria decreased significantly in either microsome or mitochondria or both from DJ-1 KO cells (Fig. 2*D*).

DJ-1 Is Part of the IP3R3-Grp75-VDAC1 Complex. Prior studies suggest that DJ-1 interacts with Grp75 (27). Given that Grp75 plays a crucial scaffolding role in the formation of the IP3R3-Grp75-VDAC1 tripartite complex that regulates ER-mitochondria tethering and calcium signaling (28), we investigated whether DJ-1 is in close apposition and interacts with the IP3R3-Grp75-VDAC1 complex. The juxtaposition between DJ-1 and each component of this tripartite complex was determined by in situ proximity ligation assay (PLA), which detects protein pairs located <40 nm away from each other (29). In wild-type (WT) M17 cells, the PLA analysis revealed a clear pattern of apposition between DJ-1 and IP3R3, between DJ-1 and Grp75, and between DJ-1 and VDAC1 (Fig. 3*A*), suggesting close colocalization of DJ-1 with each tripartite complex component. As a negative control, no PLA signals were detected in normal M17 cells when either one of these primary antibodies was omitted or between these pairs in the DJ-1 knockout cells (*SI Appendix*, Fig. S3).

We next tested whether DJ-1 physically interacts with IP3R3, Grp75, or VDAC1 by coimmunoprecipitation analysis in M17 cells. Endogenous DJ-1 was pulled down, and Grp75 can be pulled down with DJ-1. IP3R3 was also found in the DJ-1 immunoprecipitates. In fact, both Grp75 and IP3R3 were also coimmunoprecipitated with DJ-1 in MAM fraction (Fig. 3*C*), suggesting that this interaction occurs in the MAM fraction under physiological conditions. Similar experiments performed in the MAM fraction prepared from the mouse brain homogenates also showed that IP3R3 and Grp75 were coimmunoprecipitated by DJ-1 (Fig. 3*D*). In fact, VDAC1 was also detected in the DJ-1 pull-down fraction (Fig. 3*D*).

To further determine whether DJ-1 is associated with the IP3R3-Grp75-VDAC1 tripartite complex, cell lysates were prepared from M17 cells exposed to the reversible cross-linking agent DSP, and Blue-Native (BN)-polyacrylamide gel electrophoresis (PAGE) was performed. A large protein complex was clearly detected by IP3R3, Grp75, and VDAC1 antibodies, similar to the migration pattern of the IP3R3-Grp75-VDAC1 complex on BN-PAGE as previously reported (30, 31). Importantly, DJ-1 immunoreactivity was also present in this large complex (Fig. 3*E*). Such a comigration pattern between DJ-1 and the IP3R3-Grp75-VDAC1 complex was also found in the crude mitochondria (mitochondria/MAM) fraction prepared from M17 cell lysates (Fig. 3*F*). Furthermore, 2-dimensional (2D) analysis of M17 cell lysate (first dimension of BN-PAGE followed by second dimension of sodium dodecyl sulfate/PAGE) clearly revealed the presence of IP3R3, Grp75, and VDAC1 along with DJ-1 in this same large complex (Fig. 3*G*). Overall, these data collectively demonstrate that DJ-1 physically interacts with the IP3R3-Grp75-VDAC1 complex to form a macrocomplex in the MAM in a native state.

DJ-1 Ablation Disrupts the IP3R3-Grp75-VDAC1 Complex. Given the reduced ER-mitochondria association and MAM function in DJ-1 KO M17 cells (Fig. 1), we suspect that DJ-1 plays an important role in the formation/stabilization of the macrocomplex containing IP3R3-Grp75-VDAC1 at the MAM. To test this hypothesis, the formation of the IP3R3-Grp75-VDAC1 complex in the DJ-1 KO cells was first evaluated by the PLA assay. A significant decrease in both IP3R3/Grp75 PLA and IP3R3/VDAC1 PLA signals was noted in the DJ-1 KO M17 cells compared to vector-control cells (Fig. 4 *A* and *B*), suggesting a decreased IP3R3-Grp75-VDAC1 complex in the DJ-1 KO cells. Coimmunoprecipitation analysis demonstrated that significantly lower amounts of Grp75 were pulled down by IP3R3 in the DJ-1 KO

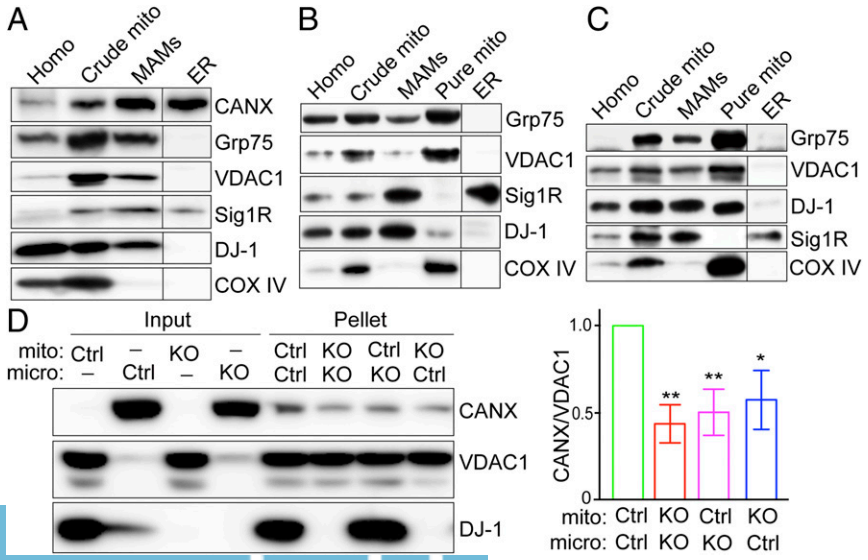

Fig. 2. DJ-1 is a MAM protein that plays a critical role in ER-mitochondria association. (*A–C*) Subcellular fractionation and immunoblot characterization of DJ-1 in the MAM fraction in normal M17 cells (*A*), WT C57BL6 mouse brain (*B*), and human cortex (*C*). Homo, total cell lysates or brain homogenates; CANX, calnexin; Sig 1R, Sigma 1R. (*D*) In vitro ER-mitochondria contact formation assay demonstrated that DJ-1 KO decreased ER binding to mitochondria. Representative immunoblot (*Left*) and quantitative analysis (*Right*) of ER bound to mitochondria in the pellets after incubation of purified mitochondria (mito) and microsome (micro) fraction from control or DJ-1 KO M17 cells. Data are means ± SD of 3 independent experiments. One-way ANOVA, $*P < 0.05$; $**P < 0.01$.

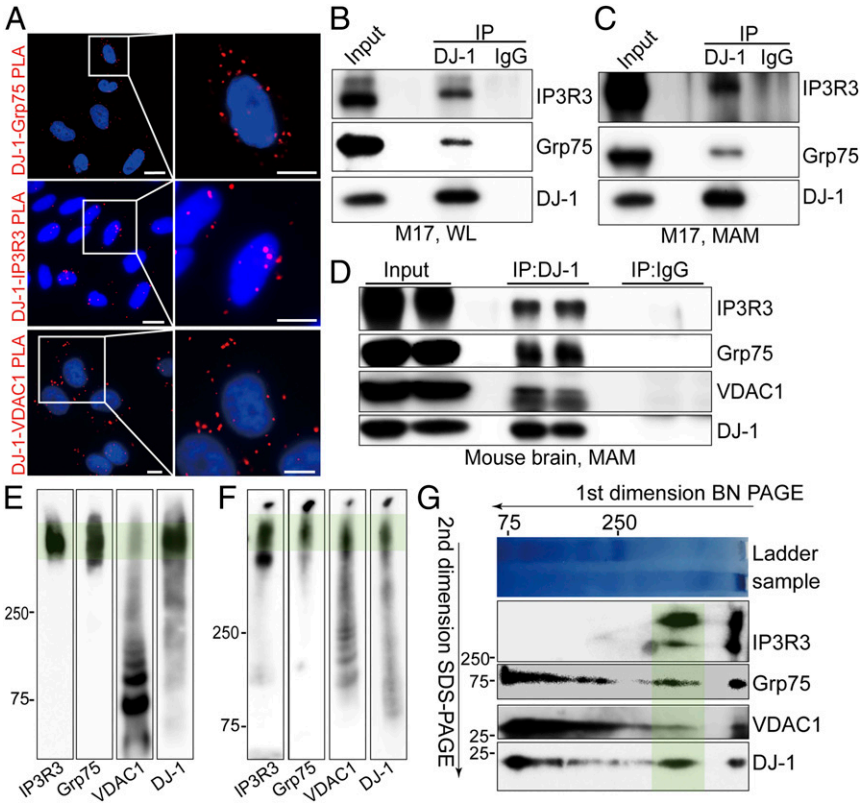

Fig. 3. DJ-1 is part of the IP3R3-Grp75-VDAC1 complex at the MAM. (*A*) In situ close association between DJ-1/Grp75 (*Top*), DJ-1/IP3R3 (*Middle*), and DJ-1/VDAC1 (*Bottom*) were determined by PLA in normal M17 cells. (Scale bar, 5 μm.) (*B–D*) Immunoblot analysis of IP3R3, Grp75, and/or VDAC1 in the DJ-1 immunoprecipitates of total lysates (*B*) and MAM fraction (*C*) from normal M17 cells or MAM fraction prepared from C57BL6 mouse brain (*D*); WL, whole lysate. (*E* and *F*) Representative BN-PAGE and immunoblot analysis of the total cell lysates (*E*) and crude mitochondrial fraction (*F*) prepared from normal M17 cells. (*G*) Representative 2D separation and immunoblot analysis of total cell lysates from normal M17 cells. In *E–G*, green shading highlights the macrocomplex that contained all 4 components. Data are representative of 3 independent experiments.

cells (Fig. 4*C*). Consistently, the BN-PAGE also revealed significantly decreased levels of the large macrocomplex recognized by IP3R3 in the DJ-1 KO cells (Fig. 4*D*).

Expression of WT but Not fPD-Associated Mutant DJ-1 Rescued DJ-1 Ablation-Induced MAM Deficits. It is believed that fPD-associated DJ-1 mutations caused loss of DJ-1 function. To explore whether fPD-associated DJ-1 mutations also caused a loss of function in the MAM regulation, we re-expressed CRISPR-resistant DJ-1 L166P mutant or WT DJ-1 in DJ-1 KO M17 cells (*SI Appendix*, Fig. S4*A*) and determined MAM-regulated mitochondrial Ca^{2+} uptake following histamine treatment (*SI Appendix*, Fig. S4*B*). Indeed, impaired mitochondrial calcium uptake upon histamine treatment in the DJ-1 KO cells was rescued by the reexpression of WT DJ-1 but not the reexpression of the L166P mutant. Similarly, mitochondrial dysfunction as measured by ATP production in the DJ-1 KO cells was also rescued by WT DJ-1 but not by L166P mutant (*SI Appendix*, Fig. S4*C*). Interestingly, despite the comparable DJ-1 expression levels, significantly reduced levels of IP3R3 and Grp75 were coimmunoprecipitated by DJ-1 in L166P-expressing DJ-1 KO cells compared to that of WT DJ-1–expressing DJ-1 KO cells (*SI Appendix*, Fig. S4*D*), suggesting a reduced interaction between the mutant DJ-1 and the IP3R3/Grp75 complex.

DJ-1 Ablation Caused IP3R3 Accumulation at the MAM. Biochemical alterations in the MAM fraction were determined by Western blot in DJ-1 KO M17 cells (Fig. 5*A*). No significant changes in the levels of Calnexin, Grp75, and VDAC1 were noted in either the total cell lysates or MAM fractions of the DJ-1 KO M17 cells. Surprisingly, increased levels of IP3R3, especially the higher-molecular-weight forms, were found in both total cell lysates and MAM factions of DJ-1 KO M17 cells (Fig. 5*A*), suggesting disturbed and possibly aggregated IP3R3 proteins in DJ-1 KO cells. Significantly decreased levels of Sigma 1R were also noted in the DJ-1 KO cells (Fig. 5*A*). Real-time PCR revealed no significant changes in the messenger RNA levels of IP3R in DJ-1 KO cells (*SI Appendix*, Fig. S5), suggesting that increased IP3R3 is likely due to a posttranslational event. We explored the possibility of IP3R3 aggregation in DJ-1 KO M17 cells by determining the levels of IP3R3 in the Nonidet P-40–soluble and –insoluble fractions from DJ-1 KO M17 cells and found that both the monomer and the higher-molecular-weight forms of IP3R3 significantly increased in the insoluble fraction of DJ-1 KO M17 cells (Fig. 5*B*), suggesting a potential disturbance in the IP3R3 degradation and turnover in DJ-1 KO cells.

IP3 binding to IP3R causes IP3R conformational changes leading to channel opening and its own ubiquitination and degradation, which is essential for the homeostasis and proper signaling of the IP3R (32–34). We then investigated the IP3R3 degradation dynamics after treatment of Carbachol (CCh), an IP3 inducer, which is widely used in inducing IP3R activation and subsequent degradation in the IP3R homeostasis studies (34). As expected, in control M17 cells, CCh treatment caused a rapid degradation of IP3R3 by 30% within 30 min, which was further reduced by 60% at 4 h. However, in great contrast, the IP3R3 levels were significantly higher in DJ-1 KO cells at basal level and remained unchanged after CCh treatment, suggesting that calcium efflux-induced IP3R3 degradation was almost entirely blocked in the DJ-1 KO M17 cells (Fig. 5*C*).

MAM Deficits in the Brain of DJ-1 Knockout Mice and Sporadic PD Patients In Vivo. To determine whether DJ-1 plays a similar role in the regulation of MAM in vivo, we first evaluated the formation of the IP3R3-Grp-75-VDAC1 complex in TH^+ neurons by the PLA assay using the IP3R3-VDAC1 pair and its costaining with TH antibody in the mouse brain (Fig. 6*A*). The IP3R3-VDAC1 PLA signal was readily observed in TH^+ neurons in the substantia nigra of WT mice but was significantly reduced in the DJ-1 KO mice. Consistently, coimmunoprecipitation analysis found significantly less Grp75 in the IP3R3 immunoprecipitates of the DJ-1 KO mouse brain homogenates (Fig. 6*B*). The BN-PAGE also confirmed significantly reduced levels of the large macrocomplex recognized by the IP3R3 in the crude mitochondrial fraction prepared from DJ-KO mouse brain (Fig. 6*C*).

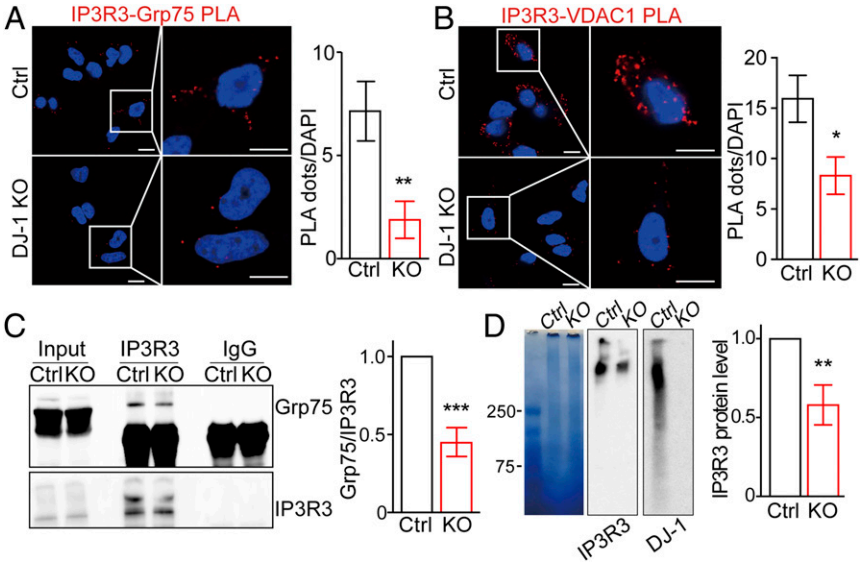

Fig. 4. DJ-1 ablation disrupted the IP3R3-Grp75-VDAC1 complex. (*A* and *B*) Representative images and quantification of PLA signals revealed decreased IP3R3-Grp75 (127 to 200 cells) and IP3R3-VDAC1 (67 to 86 cells) in DJ-1 KO cells. (Scale bar, 5 μm.) (*C*) Representative immunoblot and quantitative analysis of Grp75 coimmunoprecipitated with IP3R3 antibody in control and DJ-1 KO cells. (*D*) Representative Blue-native PAGE and immunoblot images and quantitative analysis of the macrocomplex in total cell lysates from control and DJ-1 KO cells. (*A*–*D*) Data are means ± SD based on 3 independent experiments, Student *t* test, $*P < 0.05$, $**P < 0.01$, $***P < 0.001$.

Moreover, Western blot analysis of the brain homogenates and MAM preparation revealed significantly increased levels of IP3R3, especially the higher-molecular-weight forms, along with significantly reduced Sigma 1R in the brain of DJ-1 KO mice (Fig. 6*D*). These results demonstrate MAM deficits caused by DJ-1 KO in vivo.

Western blot analysis of brain homogenates prepared from substantia nigra of patients with sporadic PD revealed significantly reduced DJ-1 levels as compared with that of age- and sex-matched controls (*SI Appendix*, Fig. S6 *A* and *B*). Interestingly, significantly increased IP3R3 and the higher-molecular-weight forms were also found in PD brain (*SI Appendix*, Fig. S6 *A* and *B*). PLA assay revealed significantly decreased IP3R3-DJ-1 PLA signals (*SI Appendix*, Fig. S6*C*) and IP3R3-VDAC1 PLA signals (*SI Appendix*, Fig. S6*D*) in neurons in the substantia nigra of PD brain.

Discussion

In this study, we focused on the role of DJ-1 in the regulation of ER-mitochondria association and presented evidence demonstrating that DJ-1 is present in the MAM. In fact, DJ-1 interacts with the well-known MAM proteins IP3R3, Grp75, and VDAC1 to form a macrocomplex at the ER-mitochondria contact sites. The loss of DJ-1 disrupted this macrocomplex and reduced the levels of the IP3R3-Grp75-VDAC1 tripartite complex both in vitro and in vivo. Consequently, DJ-1 ablation led to reduced ER-mitochondria association and disturbance in MAM function as evidenced by impaired mitochondrial calcium uptake, which could be rescued by the expression of WT DJ-1 but not fPD-associated L166P mutant DJ-1. However, DJ-1 ablation caused increased levels of IP3R3 in the cell lysates and MAM preparation. We speculate that this increase represents disturbed and possibly aggregated IP3R3 channels. This is in line with the increased levels of high-molecular-weight form of the IP3R3 as well as the increased levels of IP3R3 in the Nonidet P-40–insoluble fractions of the DJ-1 KO cells. Indeed, disturbed IP3R3 homeostasis is further supported by the impaired IP3R3 degradation and turnover after CCh treatment in the DJ-1 KO cells.

DJ-1 is mainly cytosolic. Prior studies have demonstrated the presence of mitochondrial DJ-1 and have established mitochondria as a critical site for DJ-1 function (16). In this study, we

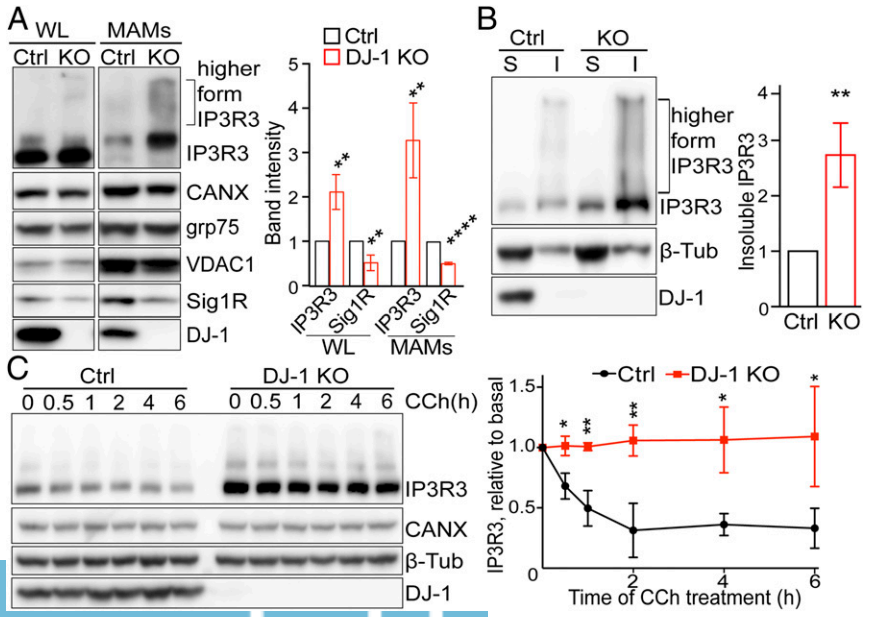

Fig. 5. DJ-1 ablation caused IP3R3 accumulation at MAM. (*A*) Representative immunoblot and quantitative analysis of MAM proteins in total cell lysates and MAM fractions from control and DJ-1 KO M17 cells. Data are normalized to calnexin. WL, whole lysate; CANX, calnexin; Sig 1R, Sigma 1R. (*B*) Representative immunoblot and quantitative analysis of IP3R3 in the detergent-soluble (S) and -insoluble (I) fractions of total cell lysates from control and DJ-1 KO M17 cells. (*C*) Representative immunoblot and quantitative analysis of time-dependent degradation of IP3R3 after treatment of CCh in control and DJ-1 KO M17 cells. Data are means ± SD from 3 independent experiments, Student *t* test; $*P < 0.05$; $**P < 0.01$; $****P < 0.0001$.

also confirmed mitochondrial and cytosolic localization of DJ-1, but further demonstrated that a subset of DJ-1 is located at the MAM fraction in M17 neuronal cells and in the mouse and human brain in vivo. This is unlikely due to the mitochondrial contamination because of the complete removal of mitochondria contents in our MAM preparation as evidenced by the absence of mitochondrial markers in the MAM fraction. MAM localization of DJ-1 is corroborated by the in situ PLA assay which clearly demonstrated close juxtaposition between DJ-1 and well-characterized MAM proteins including IP3R3, Grp75, VDAC1 (Fig. 3), and Sigma 1R. Furthermore, coimmunoprecipitation analysis confirmed physical interaction between DJ-1 and IP3R3, Grp75, and VDAC1 (Fig. 3). Therefore, our studies extend the function of DJ-1 to communication between the ER and the mitochondria at their contact sites. As a specialized structure of bidirectional communication, ER-mitochondria contacts regulate a number of essential physiological functions including Ca^{2+} signaling, phospholipid biosynthesis, autophagosome formation, mitochondrial fission/fusion and function, and cell death (8). Notably, DJ-1 has been implicated in the regulation of many of these functions. For example, DJ-1 knockdown impairs autophagy in various cell types, and both PI3K/AKT and mTORC1 pathways are involved (35, 36). Multiple groups demonstrated that manipulation of the expression of DJ-1 leads to changes in mitochondrial morphology by impacting mitochondrial fission/fusion factors including DLP1 and Mfn2 (17–19). DJ-1 is involved in the regulation of depolarization-evoked Ca^{2+} release from the sarcoplasmic reticulum and the mitochondrial permeability transition pore opening (20–22). In our study, consistent with the MAM presence of DJ-1, DJ-1 ablation caused a decrease in the physical and functional interactions between ER and mitochondria at the contact sites as demonstrated by 3 independent approaches, namely, electron microscopic and in situ PLA analysis of ER-mitochondria physical proximity and mitochondria-targeted CEPIA4-based measurement of mitochondrial calcium uptake, confirming recent studies (37). Importantly, we also found similar deficits in the brain of DJ-1 KO mice in vivo. In fact, reduced DJ-1 level and IP3R3-DJ-1 interaction were associated with reduced ER-mitochondria association in neurons in the substantia nigra in sporadic PD brain. It is therefore not unlikely that DJ-1 deficiency, through the impaired integrity and function of ER-mitochondria contacts, negatively impacts various ER-mitochondria–regulated physiological functions that may be of significance to the pathogenesis of both DJ-1–associated familial and sporadic PD. In this regard, it is interesting to note that abnormal ER-mitochondria association is increasingly implicated in neurodegenerative diseases, including PD, suggesting that abnormal ER-mitochondria association may represent a common neurodegenerative mechanism (9). For example, PINK1 and Parkin have been found in the ER-mitochondria contacts and modulate the structure and function of ER-mitochondria contacts through Mfn2 ubiquitination (24). Mutant α-synuclein disrupted the binding between ER-mitochondria–tethering proteins VAPB and PTPIP51 and perturbed mitochondrial calcium uptake and ATP production (23). On the other hand, increased ER-mitochondria association was reported in Alzheimer's disease (38, 39), suggesting that the proper ER-mitochondria association is essential to neuronal survival/function and that the detailed mechanism underlying abnormal ER-mitochondria association may be different between various diseases and needs to be sorted out separately.

To explore the mechanism underlying the role of DJ-1 in the regulation of the integrity and function of ER-mitochondria association, we confirmed the interaction between DJ-1 and Grp75 as previously reported (27). We further demonstrated that DJ-1 is also in close juxtaposition with and physically interacts with IP3R3 and VDAC1, the other 2 components of the IP3R3-Grp75-VDAC1 tripartite complex. Indeed, DJ-1 comigrates with IP3R3, Grp75, and VDAC1 in a large complex in the native state, which strongly suggests that DJ-1 is part of a MAM macrocomplex that contains the IP3R3-Grp75-VDAC1 complex. This finding of DJ-1 being part of a MAM macrocomplex is likely of both structural and functional significance. On one hand, the loss of DJ-1 led to significant reduction in the juxtaposition and physical interaction between IP3R3, Grp75, and VDAC1, suggesting the disruption of the IP3R3-Grp75-VDAC1 complex in the DJ-1 KO cells. This is confirmed by the significantly reduced levels of the large macrocomplex in the native state recognized by the IP3R3 in the blue-native gel. Therefore, these results demonstrate that DJ-1 acts as a critical component to stabilize the calcium channel formed by IP3R3 and VDAC1 between the ER and mitochondria, which is of pathogenic significance as signified by the findings that the L166P mutation caused impaired IP3R3-DJ-1 interaction and failed to rescue DJ-1 ablation-induced ER-mitochondria association and function. It is of interest to note that, like Grp75 (28), immunoprecipitation of DJ-1 could copurify both IP3R3 and VDAC1, suggesting that DJ-1 likely plays a similarly central role in setting up the protein complex with IP3R3 and VDAC1. The fact that the loss of DJ-1 impacted the IP3R3-Grp75-VDAC1 complex

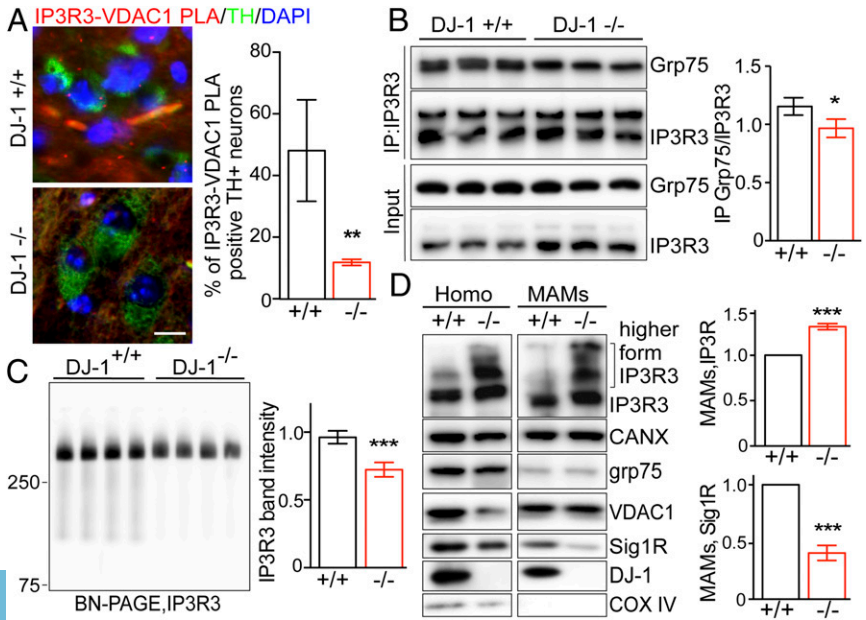

Fig. 6. DJ-1 ablation caused MAM deficits in vivo. (*A*) Representative images and quantification of IP3R3-VDAC1 PLA signals revealed decreased IP3R3-VDAC1 association in TH^+ neurons in the substantia nigra of DJ-1 KO mice. IP3R3-VDAC1 PLA (red) were developed in brain sections and costained with tyrosine hydroxylase (TH, green) (n = 3/group). (Scale bar, 20 μm.) (*B*) Representative immunoblot and quantitative analysis of Grp75 coimmunoprecipitated with IP3R3 antibody in the brain homogenates of DJ-1 KO and WT control mice (n = 3/group). (*C*) Representative BN-PAGE/immunoblot and quantitative analysis of the macrocomplex detected by IP3R3 in the crude mitochondria fraction from mouse brain homogenates (n = 4/group). (*D*) Representative immunoblot and quantitative analysis of MAM proteins, normalized to calnexin, in the brain homogenates (Homo) and MAM fractions from DJ-1 KO mice. CANX, calnexin; Sig 1R, Sigma 1R; β-Tub, β-tubulin. Data are means ± SD, Student t test; $^*P < 0.05$; $^{**}P < 0.01$; $^{***}P < 0.001$.

without affecting the MAM level of Grp75 suggests a critical role of DJ-1 that is independent of that of Grp75 in this macrocomplex. On the other hand, DJ-1 appears to have direct effects on the regulation of IP3R3 homeostasis at the ER-mitochondria contact sites since loss of DJ-1 led to accumulation of IP3R3, especially the higher-molecular-weight forms suggestive of aggregation, in the MAM fraction both in vitro and in vivo. This is further supported by the finding of a dramatic increase of IP3R3 and the higher-molecular-weight forms in the Nonidet P-40–insoluble fraction of the DJ-1 KO cells. Such a IP3R3 defect is likely the underlying cause of impaired ER release of calcium upon histamine stimulation. Binding of IP3 to IP3R causes IP3R conformational change to open the channel, and calcium efflux through IP3R causes further conformational change of IP3R that exposes its ubiquitin modification sites. This allows subsequent ubiquitination and degradation so that the IP3R protein level is fine-tuned (32–34). This fast turnover of IP3R is of great significance for the maintenance of the sensitivity of the receptor and calcium signaling. Consistent with the notion that loss of DJ-1 disrupts the homeostasis of IP3R3, IP3R3 degradation induced by CCh (34), an IP3 inducer, as observed in the control cells, was entirely blocked in the DJ-1 KO cells. Given the increased IP3R3 in the MAM fraction prepared from PD brain tissues, IP3R3 dyshomeostasis likely contributes to PD deficits. How DJ-1 interacts and regulates IP3R3 homeostasis obviously warrants further investigation. In this regard, it is of interest to note that the Sigma 1 receptor, a MAM protein involved in the stability and channel function of IP3R3 (40), is also significantly reduced after DJ-1 KO both in vitro and in vivo.

In summary, we have demonstrated that DJ-1 is localized to MAM and interacts and comigrates with the IP3R3-Grp75-VDAC1 complex. Loss of DJ-1 disrupts the IP3R3-Grp75-VDAC1 complex and IP3R3 homeostasis, which leads to decreased ER-mitochondria association and function. Our study identifies DJ-1 as a critical component of the macrocomplex containing IP3R3-Grp75-VDAC1 at the ER-mitochondria contact sites and as playing an important role in the regulation of the integrity and function of ER-mitochondria association both in vitro and in vivo. Thus, we offer insights into the cellular mechanism regulating calcium cross-talk between ER and mitochondria and the potential pathogenic mechanism of DJ-1 deficiency in PD.

Materials and Methods

Animals and Animal Care. WT and DJ-1 KO (#006577-B6.Cg-Park7tm1Shn/J) C57BL6 mice were from The Jackson Laboratory. The animal experiments were performed according to protocols approved by the Animal Care and Use Committee of Case Western Reserve University. A detailed description of materials and methods is provided in *SI Appendix*.

Data Availability. All data are included in the manuscript and *SI Appendix*.

ACKNOWLEDGMENTS. This work was partly supported by NIH Grants AG049479, NS083498, and NS083385 (to X.Z.); Alzheimer's Association Grant AARG-16-443584 (to X.Z.); and Chinese National Natural Science Fund Grants 81430022, 81971187, and 81771374 (to S.C.) and 81873778 and 81501097 (to J.L.).

1. J. A. Obeso *et al*., Past, present, and future of Parkinson's disease: A special essay on the 200th anniversary of the shaking palsy. *Mov. Disord.* **32**, 1264–1310 (2017).
2. M. H. Yan, X. Wang, X. Zhu, Mitochondrial defects and oxidative stress in Alzheimer disease and Parkinson disease. *Free Radic. Biol. Med.* **62**, 90–101 (2013).
3. Z. D. Zhou, T. Selvaratnam, J. C. T. Lee, Y. X. Chao, E. K. Tan, Molecular targets for modulating the protein translation vital to proteostasis and neuron degeneration in Parkinson's disease. *Transl. Neurodegener.* **8**, 6 (2019).
4. I. Martin, V. L. Dawson, T. M. Dawson, Recent advances in the genetics of Parkinson's disease. *Annu. Rev. Genomics Hum. Genet.* **12**, 301–325 (2011).
5. X. Reed, S. Bandrés-Ciga, C. Blauwendraat, M. R. Cookson, The role of monogenic genes in idiopathic Parkinson's disease. *Neurobiol. Dis.* **124**, 230–239 (2019).
6. P. Maiti, J. Manna, G. L. Dunbar, Current understanding of the molecular mechanisms in Parkinson's disease: Targets for potential treatments. *Transl. Neurodegener.* **6**, 28 (2017).
7. S. Paillusson *et al*., There's something wrong with my MAM: The ER-mitochondria axis and neurodegenerative diseases. *Trends Neurosci.* **39**, 146–157 (2016).
8. H. Wu, P. Carvalho, G. K. Voeltz, Here, there, and everywhere: The importance of ER membrane contact sites. *Science* **361**, eaan5835 (2018).
9. Y. Liu, X. Zhu, Endoplasmic reticulum-mitochondria tethering in neurodegenerative diseases. *Transl. Neurodegener.* **6**, 21 (2017).
10. M. Krols *et al*., Mitochondria-associated membranes as hubs for neurodegeneration. *Acta Neuropathol.* **131**, 505–523 (2016).
11. C. Guardia-Laguarta *et al*., α-Synuclein is localized to mitochondria-associated ER membranes. *J. Neurosci.* **34**, 249–259 (2014).
12. T. Calì, D. Ottolini, A. Negro, M. Brini, Enhanced parkin levels favor ER-mitochondria crosstalk and guarantee Ca(2+) transfer to sustain cell bioenergetics. *Biochim. Biophys. Acta* **1832**, 495–508 (2013).
13. C. A. Gautier *et al*., The endoplasmic reticulum-mitochondria interface is perturbed in PARK2 knockout mice and patients with PARK2 mutations. *Hum. Mol. Genet.* **25**, 2972–2984 (2016).
14. V. Gelmetti *et al*., PINK1 and BECN1 relocalize at mitochondria-associated membranes during mitophagy and promote ER-mitochondria tethering and autophagosome formation. *Autophagy* **13**, 654–669 (2017).
15. T. Calì, D. Ottolini, A. Negro, M. Brini, α-Synuclein controls mitochondrial calcium homeostasis by enhancing endoplasmic reticulum-mitochondria interactions. *J. Biol. Chem.* **287**, 17914–17929 (2012).
16. L. Zhang *et al*., Mitochondrial localization of the Parkinson's disease related protein DJ-1: Implications for pathogenesis. *Hum. Mol. Genet.* **14**, 2063–2073 (2005).
17. K. J. Thomas *et al*., DJ-1 acts in parallel to the PINK1/parkin pathway to control mitochondrial function and autophagy. *Hum. Mol. Genet.* **20**, 40–50 (2011).
18. X. Wang *et al*., Parkinson's disease-associated DJ-1 mutations impair mitochondrial dynamics and cause mitochondrial dysfunction. *J. Neurochem.* **121**, 830–839 (2012).
19. I. Irrcher *et al*., Loss of the Parkinson's disease-linked gene DJ-1 perturbs mitochondrial dynamics. *Hum. Mol. Genet.* **19**, 3734–3746 (2010).
20. A. Shtifman, N. Zhong, J. R. Lopez, J. Shen, J. Xu, Altered Ca2+ homeostasis in the skeletal muscle of DJ-1 null mice. *Neurobiol. Aging* **32**, 125–132 (2011).
21. E. Giaime, H. Yamaguchi, C. A. Gautier, T. Kitada, J. Shen, Loss of DJ-1 does not affect mitochondrial respiration but increases ROS production and mitochondrial permeability transition pore opening. *PLoS One* **7**, e40501 (2012).
22. G. Martella *et al*., Altered profile and D2-dopamine receptor modulation of high voltage-activated calcium current in striatal medium spiny neurons from animal models of Parkinson's disease. *Neuroscience* **177**, 240–251 (2011).
23. S. Paillusson *et al*., α-Synuclein binds to the ER-mitochondria tethering protein VAPB to disrupt Ca^{2+} homeostasis and mitochondrial ATP production. *Acta Neuropathol.* **134**, 129–149 (2017).
24. V. Basso *et al*., Regulation of ER-mitochondria contacts by Parkin via Mfn2. *Pharmacol. Res.* **138**, 43–56 (2018).
25. A. Sugiura *et al*., MITOL regulates endoplasmic reticulum-mitochondria contacts via Mitofusin2. *Mol. Cell* **51**, 20–34 (2013).
26. S. Watanabe *et al*., Mitochondria-associated membrane collapse is a common pathomechanism in SIGMAR1- and SOD1-linked ALS. *EMBO Mol. Med.* **8**, 1421–1437 (2016).
27. I. Tai-Nagara, S. Matsuoka, H. Ariga, T. Suda, Mortalin and DJ-1 coordinately regulate hematopoietic stem cell function through the control of oxidative stress. *Blood* **123**, 41–50 (2014).
28. G. Szabadkai *et al*., Chaperone-mediated coupling of endoplasmic reticulum and mitochondrial Ca2+ channels. *J. Cell Biol.* **175**, 901–911 (2006).
29. O. Söderberg *et al*., Direct observation of individual endogenous protein complexes in situ by proximity ligation. *Nat. Methods* **3**, 995–1000 (2006).
30. L. Gomez *et al*., The SR/ER-mitochondria calcium crosstalk is regulated by GSK3β during reperfusion injury. *Cell Death Differ.* **23**, 313–322 (2016).
31. M. Paillard *et al*., Depressing mitochondria-reticulum interactions protects cardiomyocytes from lethal hypoxia-reoxygenation injury. *Circulation* **128**, 1555–1565 (2013).
32. C. D. Bhanumathy, S. K. Nakao, S. K. Joseph, Mechanism of proteasomal degradation of inositol trisphosphate receptors in CHO-K1 cells. *J. Biol. Chem.* **281**, 3722–3730 (2006).
33. K. J. Alzayady, R. J. Wojcikiewicz, The role of Ca2+ in triggering inositol 1,4,5-trisphosphate receptor ubiquitination. *Biochem. J.* **392**, 601–606 (2005).
34. C. C. Zhu, R. J. Wojcikiewicz, Ligand binding directly stimulates ubiquitination of the inositol 1, 4,5-trisphosphate receptor. *Biochem. J.* **348**, 551–556 (2000).
35. G. Krebiehl *et al*., Reduced basal autophagy and impaired mitochondrial dynamics due to loss of Parkinson's disease-associated protein DJ-1. *PLoS One* **5**, e9367 (2010).
36. Y. Nash, E. Schmukler, D. Trudler, R. Pinkas-Kramarski, D. Frenkel, DJ-1 deficiency impairs autophagy and reduces alpha-synuclein phagocytosis by microglia. *J. Neurochem.* **143**, 584–594 (2017).
37. D. Ottolini, T. Calì, A. Negro, M. Brini, The Parkinson disease-related protein DJ-1 counteracts mitochondrial impairment induced by the tumour suppressor protein p53 by enhancing endoplasmic reticulum-mitochondria tethering. *Hum. Mol. Genet.* **22**, 2152–2168 (2013).
38. E. Area-Gomez *et al*., Upregulated function of mitochondria-associated ER membranes in Alzheimer disease. *EMBO J.* **31**, 4106–4123 (2012).
39. M. D. Tambini *et al*., ApoE4 upregulates the activity of mitochondria-associated ER membranes. *EMBO Rep.* **17**, 27–36 (2016).
40. T. Hayashi, T. P. Su, Sigma-1 receptor chaperones at the ER-mitochondrion interface regulate Ca(2+) signaling and cell survival. *Cell* **131**, 596–610 (2007).